Dynamical Model Development and Parameter Identification for an Anaerobic Wastewater Treatment Process

Olivier Bernard,[1] Zakaria Hadj-Sadok,[1] Denis Dochain,[2] Antoine Genovesi,[3] Jean-Philippe Steyer[3]

[1]INRIA, COMORE Project, BP93, 06902 Sophia-Antipolis Cedex, France; telephone: +33 492 38 77 85; fax: +33 492 38 78 58; e-mail: obernard@sophia.inria.fr
[2]CESAME-UCL, Av G. Lemaître, 4-6, 1348 Louvain-La-Neuve, Belgium
[3]LBE-INRA, Av des Etangs, 11100 Narbonne, France

Received 26 December 2000; accepted 11 June 2001

Abstract: This paper deals with the development and the parameter identification of an anaerobic digestion process model. A two-step (acidogenesis–methanization) mass-balance model has been considered. The model incorporates electrochemical equilibria in order to include the alkalinity, which has to play a central role in the related monitoring and control strategy of a treatment plant. The identification is based on a set of dynamical experiments designed to cover a wide spectrum of operating conditions that are likely to take place in the practical operation of the plant. A step by step identification procedure to estimate the model parameters is presented. The results of 70 days of experiments in a 1-m^3 fermenter are then used to validate the model. © 2001 John Wiley & Sons, Inc. *Biotechnol Bioeng* **75**: 424–438, 2001.
Keywords: anaerobic digestion; dynamical modeling; model identification

INTRODUCTION

The anaerobic wastewater treatment process presents very interesting advantages compared to the classical aerobic treatment (Mata-Alvarez et al., 2000; Pavlostathis, 1994): It has a high capacity to degrade concentrated and difficult substrates (plant residues, animal wastes, food industry wastewater, and so forth), produces very few sludges, requires little energy, and, in some cases, it can even recover energy using methane combustion. But in spite of these advantages, the anaerobic treatment plants are still very rare at the industrial scale, probably because they are known to become easily unstable under some circumstances, such as variations of the process operating conditions (Fripiat et al., 1984). Nevertheless, this drawback can be overcome by associating a monitoring procedure with a decision support system that allows enhancement of the stable performance of the online wastewater treatment operation via a feedback control loop (Dochain et al., 1991; Perrier and Dochain, 1993; Steyer et al., 1999). Therefore, a reliable dynamic model of the process is required for the design of such monitoring and control algorithms.

The dynamical modeling of anaerobic digestion has been an active research area during the last three decades. Andrews (1968) introduced the Haldane model to characterize growth inhibition that can emphasize the process instability (i.e., the biomass wash-out via the accumulation of acids). A model with a single bacterial population was then proposed (Graef and Andrews, 1974).

The representation of the process was then improved by considering three stages: solubilization of organics, acidogenesis, and methanogenesis (Hill and Barth, 1977). Mosey (1983) introduced a four-population model with two acidogenesis reactions and two methanization reactions which also emphasizes the role of hydrogen. These main modeling studies have then been extended and detailed by other authors in order to get closer to the complexity of the process (Moletta et al., 1986; Batstone et al., 1997; Costello et al., 1991a; Costello et al., 1991b; Fernandes et al., 1993; Kiley et al., 1997). It results in detailed models of the process which include several bacterial populations and several substrates. As a result, the number of parameters in these models can become very large.

As suggested in the above paragraph, there exists a wide range of models dealing with anaerobic digestion. However, the models describing with detail all the processes responsible for anaerobic digestion are generally difficult to use for control purposes (Bastin and Dochain, 1990). In addition, the question of model identification and validation is rarely performed in a sufficiently large range of operating conditions (typically, loading rates and retention times). Moreover, in all these models, the considered process is often assumed to behave like a continuously stirred tank reactor (CSTR). In practice, the technologies often aim at increasing the contact surface between the biological phase and the organic matter in order to improve the process efficiency. As a consequence, the technology

Correspondence to: Olivier Bernard

© 2001 John Wiley & Sons, Inc.

based on fixed or fluidized bed reactors generate a triphasic medium (solid–liquid–gas) where the bacteria are usually not in the liquid phase anymore. The principles of CSTR modeling (i.e., liquid homogeneous medium) may thus not be valid anymore in these reactors.

However, the lack of phenomenological knowledge, the complexity of the process, its nonlinear nature, and the lack of sensors explain why most of the existing models are generally only rough approximations that have not been validated with a large set of data. In this context, it is of great interest to derive models that would be as insensitive as possible to the lack of phenomenological knowledge. The model based on mass-balance considerations circumvents this difficulty by locating the biological lack of knowledge in dedicated terms; namely, the reaction rates. The use of such models for monitoring and control design has proved to be effective (Bastin and Dochain, 1990), because they minimize the number of assumptions in the model-building exercise.

Let us now recall that a dynamical model can be used for different purposes. One objective can be the numerical simulation of the process behavior; for example, for predicting its dynamical behavior or for identifying and understanding better the major mechanisms driving its dynamics. Another objective is the design of monitoring and control algorithms. The current work has to be viewed in the latter context. The proposed model has been developed within the framework of a European Economic Community project (AMOCO, FAIR program) that is aimed at developing a monitoring and control system for anaerobic digestion processes. The proposed model is inspired form the model of Graef and Andrews (1974), but it has been modified to lead to better (and simpler) structural properties. Moreover, a second bacterial population has been introduced to better reproduce the destabilization phase. In this paper, we present in detail the modeling of the gaseous flow rates with respect to the biological and chemical species in the fermenter. This leads to a gaseous flow rate description that differs from most of the previous models published in the literature. Moreover, we have considered a simple model for bacterial attachment. Another important original aspect of the current work is the calibration procedure of the model parameters with experimental data at equilibrium. The experiments used for model building and identification have been carefully chosen so as to correspond to a sufficiently wide range of operating conditions assumed to be possibly encountered in the practical operation of a treatment plant. Secondly, as with any systematic identification study, the model parameter calibration has followed two steps: parameter identification, then model validation. These two steps have been performed on different data sets, and the model performance during transient conditions is evaluated during the validation step.

The paper is organized as follows. The first section briefly describes the anaerobic digestion fixed-bed reactor, the measurement devices, and the considered methods. The modeling assumptions are then introduced in a second section. We simplify the process by considering two main bacterial populations: X_1, the acidogenic bacteria population, and X_2, the methanogenic bacteria population. We then give a description of the basic elements of the model (reaction network, chemical equilibria, hydrodynamics). From these considerations, a mass-balance-based model consisting of a set of six differential equations is derived. The equilibrium points of this model are studied in the following section, the main objective being to emphasize the role played by each parameter. These results are then applied in another section to calibrate and validate the model using experimental data produced by a 1-m^3 fixed-bed fermenter located at the LBE-INRA (Narbonne, France). The parameters of the model are identified on the basis of a set of steady-state data. The mass-balance model is then validated in the last section using experimental data from a wide range of operating conditions covering 3 months of process operation.

MATERIALS AND METHODS

The Influent

The experiments were performed with raw industrial wine distillery vinasses obtained from local wineries in the area of Narbonne, France. This substrate, neither sterile nor homogeneous, is stored in three tanks (27 m^3 each) that are connected to the reactor by a piping system of about 0.5 m^3. The characteristics of the effluent in those tanks and in the pipes are given in Table I.

The Reactor

The pilot plant is an anaerobic upflow fixed-bed digester. The reactor is a circular column of 3.5-m height and 0.6-m diameter. The effective volume of the medium is 0.948 m^3. The support surface equals 135 m^2 (Cloisonyl: 180

Table I. Characteristics of the industrial wine distillery wastewater.

Component	Range
Volatile Fatty Acids (g/L)	[5.00–6.00]
% acetic	[35–55]
% propionic	[15–30]
% butyric	[15–35]
% isobutyric	[0–1]
% pentanoic	[5–15]
% isopentanoic	[0–0.1]
Total organic carbon (g/L)	[2.50–6.00]
Total COD (g/L)	[9.00–17.4]
Soluble COD (g/L)	[7.60–16.0]
Total suspended solids (g/L)	[2.40–5.00]
Volatile suspended solids (g/L)	[1.20–2.70]
Alkalinity (mEq/L)	[30.8–62.4]
pH	[5.00–5.40]

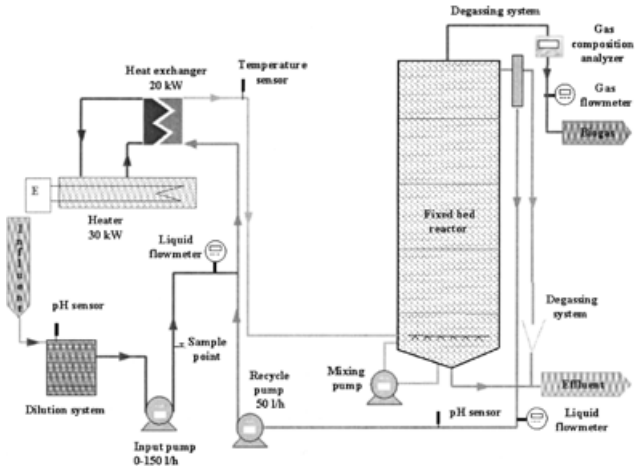

Figure 1. Schematic view of the fixed-bed anaerobic digester (LBE-INRA, Narbonne, France).

m^2/m^3). The dilution of the influent is performed by adding water to 20 L of vinasses (measured with the flowmeter) in a 200-L tank. The feeding tanks are equipped with level sensors that allows obtaining of a selected concentration in the influent. The pH is measured and controlled in the feeding tank. Figure 1 describes the pilot plant and the measurement devices.

The Online Measurements

The temperature inside the reactor is controlled at 35°C. The temperature regulation is performed in the recycle loop via an electric heater using a PID controller. The influent flow rate is measured by an electromagnetic sensor (Khrone).

The gas analysis loop (see Fig. 1) consists of a dryer that eliminates the humidity by cooling the gas. The Ultramat 22P sensor (Siemens) measures the CO_2/CH_4 percentage of the analyzed gas. The gas flowmeter is located at the output of the loop. It uses an electromagnetic floater to continuously measure the produced gas flow rate.

The Offline Measurements

The samples used to determine the concentrations in the inlet are taken in the pipe just after the feeding pump. The samples for the outlet concentrations are taken just before their rejection to the sewer. The samples are stored at 4°C. The dissolved part is obtained after centrifugation for 15 min at 15,000 rpm.

Measurement of Total Suspended Solids (TSS) and Volatile Suspended Solids (VSS)

The residue from centrifugation is put in the steam room (105°C) in a 30-ml weighted ceramic pot. Twenty-four hours later, the pot is weighed precisely (TSS measurement, NF T 90-029) and then put in a furnace at 550°C for 2 h. The pot is weighed again. The difference between both weights gives the VSS (NF T 90-105-2).

Measurement of the Volatile Fatty Acids (VFA) Concentration

The VFA are measured with a gas chromatograph (Fisons Instruments GC8000) equipped with an Econocap FFAP (Alltech) column with a length of 15 m, 1.2 μm film width, 250°C maximum temperature, and regeneration at 200°C overnight.

The centrifuged samples are diluted to the external standard scale and mixed with the same volume of the internal standard (ethyl 2 butyric acid 1 g/L, acidified to 5% with H_3PO_4). The programmed method allows the total separation of the VFA.

Measurement of the Chemical Oxygen Demand (COD)

The principle of chemical oxygen demand (COD) measurement (NF T 90-101) is the oxidation of the organic matter by a potassium bichromate excess, in acid media (H_2SO_4) at boiling temperature. The oxidant excess is titrated by a reducing solution of Mohr salt (ammonium and ferrum sulfate).

Measurement of the Alkalinity

Acid (HCl) is added to the sample in order to reach pH = 5.75 (the volume titrated corresponds to partial alkalinity). Then, acid is added again until the pH reaches the value of 4.3 and the total added acid volume is the total alkalinity. The concentration of acetate and bicarbonate can be determined from partial and total alkalinity (Ripley et al., 1986).

The Experimental Protocol

The experimental protocol has been determined in order to cover a wide range of organic loading rates and to obtain situations close to the destabilization of the fermenter. This is performed via consecutive step variation of both the dilution rate and the influent COD. They are maintained constant for a sufficiently long period of time in order to reach a steady state. The influent time evolutions are presented in Fig. 2. Note that some failures (leaks, pump failures, tube clogging, and so forth) have slightly disturbed the initial protocol.

MODEL ASSUMPTIONS AND DESCRIPTION

Model Assumptions

The choice of the number of considered bacterial populations involved in the anaerobic digestion process is

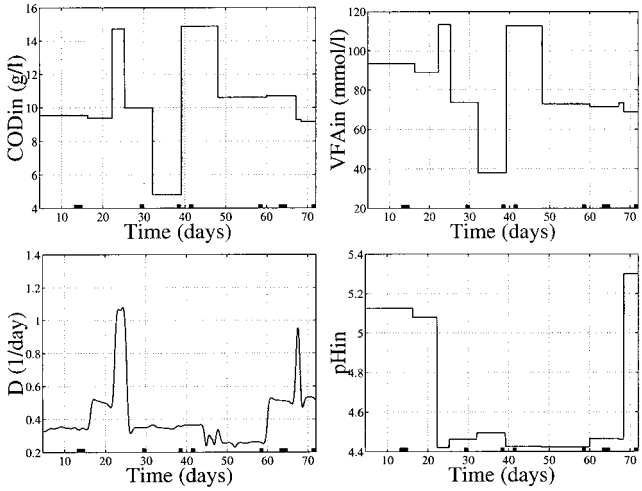

Figure 2. Influent profiles during the experiment. The values of COD, VFA, and pH are extrapolated for any time from offline measurements. The values of the dilution rate result from online measurements. The time periods used for the parameter identification are represented with a thick line on the time axis.

directly linked to the model complexity. As one of our objectives is to obtain a model that would be able to represent the destabilization phenomenon while being identifiable, we assume that the bacterial populations can be divided into two main groups of homogeneous characteristics, and that the anaerobic digestion can be described by a two-stage process. In the first step (acidogenesis), the acidogenic bacteria (X_1) consume the organic substrate (S_1) and produce CO_2 and volatile fatty acids (S_2). The population of methanogenic bacteria (X_2) uses, in a second step, the volatile fatty acids as substrate for growth, and produce CO_2 and methane.

On the basis of hydrodynamical tests, we assume that the reactor behaves like a perfectly mixed tank, and that the biomass is uniformly distributed within the reactor.

Biological Reaction Pathways

The acidogenic and methanogenic bacteria intervene in the two following biological reactions:

- Acidogenesis (with reaction rate $r_1 = \mu_1 X_1$):

$$k_1 S_1 \xrightarrow{r_1} X_1 + k_2 S_2 + k_4 CO_2 \tag{1}$$

- Methanization (with reaction rate $r_2 = \mu_2 X_2$):

$$k_3 S_2 \xrightarrow{r_2} X_2 + k_5 CO_2 + k_6 CH_4 \tag{2}$$

S_1 represents the organic substrate (and its concentration) characterized by its COD (g/L). The total concentration of VFA is denoted S_2 (mmole/L). In the sequel, we assume that S_2, which is mainly composed of acetate, propionate, and butyrate, basically behaves like pure acetate. It is important to note that the total COD is composed of S_1 and S_2. μ_1 and μ_2 (d^{-1}) represent the specific growth rates of acidogenesis and methanization, respectively.

Chemical Species

The Inorganic Carbon

Let us consider the chemical reactions involving the inorganic carbon mainly composed of dissolved CO_2, bicarbonate (B), and carbonate in line with Rozzi (1984). In normal operating conditions, the pH range is between 6 to 8, and the temperature is between 35 and 38°C. In those conditions, the affinity constant for carbonate/bicarbonate ($K_c = 4.7 \times 10^{-11}$ mol/L) indicates that the carbonate concentration will remain negligible compared to the bicarbonate. The total inorganic carbon C in the considered pH range is then approximately equal to:

$$C = CO_2 + B \tag{3}$$

and the bicarbonate and dissolved CO_2 concentrations are determined by the following chemical reaction (H^+ are the protons):

$$B + H^+ \rightleftharpoons CO_2 + H_2O \tag{4}$$

we denote K_b the affinity constant of this reaction ($K_b = 6.5 \times 10^{-7}$ mol/L):

$$K_b = \frac{[H^+]B}{CO_2} \tag{5}$$

The Volatile Fatty Acids

The total concentration of VFA is composed of ions S^- (mainly acetate) and un-ionized SH (mainly acetic acid):

$$S_2 = [SH] + [S^-] \tag{6}$$

The corresponding affinity constant is equal to:

$$K_a = \frac{[H^+][S^-]}{[SH]} \tag{7}$$

The numerical value of K_a in the considered pH range ($K_a = 1.5 \times 10^{-5}$ mol/L) shows that $[SH]$ is negligible and therefore:

$$S_2 \simeq [S^-] \tag{8}$$

The Ion Balance

The total alkalinity Z is defined as the sum of dissociated acids in the medium:

$$Z = B + [S^-] \tag{9}$$

From Eq. (8), we have in the considered pH range:

$$Z \simeq B + S_2 \tag{10}$$

Remark: This assumption is not valid in the influent wastewater, where the pH can be very low. We must therefore compute the influent alkalinity with respect to the influent bicarbonate (B_{in}) and VFA (S_{2in}) as follows:

$$Z_{in} = B_{in} + \frac{K_a}{K_a + 10^{-pH}} S_{2in} \tag{11}$$

Note also that B_{in} is negligible at low pH.

We assume that all the other anions (of concentration denoted Z_0) that significantly influence the total concentration of anions in the medium (i.e., $Z + Z_0$) are not affected by the anaerobic digestion process. Therefore, Z_0 does not vary between the influent wastewater and the medium in the fermenter: $dZ_0/dt = 0$. In the considered pH range, it is generally the case, because $[OH^-]$, $[H_2CO_3^-]$, and $[CO_3^{2-}]$ are negligible compared to B and S_2, so that $Z_0 \simeq 0$. In some particular cases, chloride can be in high concentrations and significantly contribute to the total concentration of anions, and then $Z_0 \simeq [Cl^-]$. Our hypothesis then means that the chloride concentration is not modified in the reactor.

From the electric balance of the charges in the medium, $Z + Z_0$ represents also the total concentration of cations.

The Gases

We assume that the gas outflow is mainly composed of CO_2 and CH_4. Because of the very low solubility of methane, the concentration of dissolved methane is neglected and the produced methane is assumed to go directly out of the fermenter with a molar flow rate q_M proportional to the reaction rate of methanogenesis:

$$q_M = k_6 \mu_2 X_2 \tag{12}$$

For the outflow rate of CO_2, we must take the storage of CO_2 in the total inorganic carbon compartment into account. The molar CO_2 flow rate q_C can be computed using Henry's law:

$$q_C = k_L a(CO_2 - K_H P_C) \tag{13}$$

with $k_L a$ being the liquid–gas transfer coefficient, K_H being Henry's constant, and P_C being the CO_2 partial pressure.

If we assume that the gas pressures rapidly reach their equilibrium, we get a relationship between the partial pressure and the flow rates from the ideal gas law:

$$\frac{P_T - P_C}{q_M} = \frac{P_C}{q_C} \tag{14}$$

where P_T is the total pressure in the fermenter (typically corresponding to the atmospheric pressure).

From Eqs. (13) and (14), we have:

$$K_H P_C^2 - \phi P_C + P_T CO_2 = 0 \tag{15}$$

with

$$\phi = CO_2 + K_H P_T + \frac{q_M}{k_L a} \tag{16}$$

Let us compute the roots of Eq. (15), which is of the form $\pi(P_C) = 0$, where π is a binomial equation. First, note that:

$$\pi(P_T) = -\frac{P_T q_M}{k_L a} < 0 \tag{17}$$

This shows that the largest root of Eq. (15) is larger than P_T, and therefore is not a physically admissable solution. The only admissible solution is thus the lowest root of Eq. (15); that is:

$$P_C = \frac{\phi - \sqrt{\phi^2 - 4K_H P_T CO_2}}{2K_H} \tag{18}$$

Finally, the CO_2 concentration can be computed by combining Eqs. (3) and (10):

$$CO_2 = C + S_2 - Z \tag{19}$$

The Hydrodynamics of the Fermenter

Additional experiments have shown that the recirculation rate is high enough to maintain the fermenter in homogeneous conditions. As a consequence, the dynamics of the chemical species are directly influenced by the dilution rate D of the fermenter (defined as the ratio of the influent flow rate over the volume of the fermenter).

For a fixed-bed reactor, the biomass is attached on a support. It is therefore not affected by the dilution effect as in a CSTR. Nevertheless, some bacteria do not fix on their support or are detached by the liquid flow. Thus, we decided to incorporate this effect in the hydrodynamical modeling of the biomass. In order to keep a simple mathematical description of the process, we simply consider that only a fraction α of the biomass is in the liquid phase. The parameter α ($0 \le \alpha \le 1$) therefore reflects this process heterogeneity: $\alpha = 0$ corresponds to an ideal fixed-bed reactor, whereas $\alpha = 1$ corresponds to an ideal CSTR.

THE MASS-BALANCE MODEL

Let us denote by $\xi = [X_1, X_2, Z, S_1, S_2, C]^T$ the vector of model variables (^{T}denotes the transpose operator). From the considerations of reactions (1), (2), and (4), we obtain the following mass-balance model:

$$\frac{dX_1}{dt} = [\mu_1(\xi) - \alpha D]X_1 \tag{20}$$

$$\frac{dX_2}{dt} = [\mu_2(\xi) - \alpha D]X_2 \tag{21}$$

$$\frac{dZ}{dt} = D(Z_{in} - Z) \tag{22}$$

$$\frac{dS_1}{dt} = D(S_{1in} - S_1) - k_1\mu_1(\xi)X_1 \tag{23}$$

$$\frac{dS_2}{dt} = D(S_{2in} - S_2) + k_2\mu_1(\xi)X_1 - k_3\mu_2(\xi)X_2 \tag{24}$$

$$\frac{dC}{dt} = D(C_{in} - C) - q_C(\xi) + k_4\mu_1(\xi)X_1 + k_5\mu_2(\xi)X_2 \tag{25}$$

with

$$q_C(\xi) = k_L a[C + S_2 - Z - K_H P_C(\xi)] \tag{26}$$

where $P_C(\xi)$ is computed from Eqs. (12), (16), (18), and (19) as follows:

$$P_C(\xi) = \frac{\phi - \sqrt{\phi^2 - 4K_H P_T(C + S_2 - Z)}}{2K_H} \tag{27}$$

with

$$\phi = C + S_2 - Z + K_H P_T + \frac{k_6}{k_L a}\mu_2(\xi)X_2$$

S_{1in} (g COD/L), S_{2in} (mmole/L), C_{in} (mmole/L), and Z_{in} (mmole/L) are the influent concentrations of S_1, S_2, C, and Z, respectively.

Moreover, we have the following model equations for the methane gas flow rate and for the pH from Eq. (12) and Eqs. (7), (10), and (19):

$$q_M(\xi) = k_6\mu_2(\xi)X_2 \tag{28}$$

$$\mathrm{pH}(\xi) = -\log_{10}\left(K_b\frac{C - Z + S_2}{Z - S_2}\right) \tag{29}$$

The model can then be rewritten in a more general matrix form:

$$\frac{d\xi}{dt} = Kr(\xi) - D\xi - Q + F \tag{30}$$

where

$$\xi = \begin{bmatrix} X_1 \\ X_2 \\ Z \\ S_1 \\ S_2 \\ C \end{bmatrix}, \quad r(\xi) = \begin{bmatrix} \mu_1(\xi)X_1 \\ \mu_2(\xi)X_2 \end{bmatrix}, \quad K = \begin{bmatrix} 1 & 0 \\ 0 & 1 \\ 0 & 0 \\ -k_1 & 0 \\ k_2 & -k_3 \\ k_4 & k_5 \end{bmatrix} \tag{31}$$

$$F = \begin{bmatrix} 0 \\ 0 \\ DZ_{in} \\ DS_{1in} \\ DS_{2in} \\ DC_{in} \end{bmatrix}, \quad Q = \begin{bmatrix} 0 \\ 0 \\ 0 \\ 0 \\ 0 \\ q_C(\xi) \end{bmatrix},$$

$$D = \begin{bmatrix} \alpha D & 0 & 0 & 0 & 0 & 0 \\ 0 & \alpha D & 0 & 0 & 0 & 0 \\ 0 & 0 & D & 0 & 0 & 0 \\ 0 & 0 & 0 & D & 0 & 0 \\ 0 & 0 & 0 & 0 & D & 0 \\ 0 & 0 & 0 & 0 & 0 & D \end{bmatrix} \tag{32}$$

The model given by Eq. (30) will serve as a basis for the design of online monitoring and control strategies of the anaerobic digestion process (Bastin and Dochain, 1990). For this purpose, the modeling of the growth rates $\mu_1(\xi)$ and $\mu_2(\xi)$ is not required. Yet, for numerical simulations, analytical expressions for the growth rates are needed. In the following section, expressions for $\mu_1(\xi)$ and $\mu_2(\xi)$ are proposed.

Modeling of the Bacterial Kinetics

The modeling of biological kinetics is a difficult task for which a systematic methodology is still lacking. For the sake of model simplicity, and in line with other works on anaerobic digestion modeling, we shall consider the following models for bacterial kinetics.

Acidogenic Bacteria

We consider Monod-type kinetics for the growth of acidogenic bacteria; that is:

$$\mu_1(S_1) = \mu_{1max}\frac{S_1}{S_1 + K_{S1}} \tag{33}$$

where μ_{1max} is the maximum bacterial growth rate, and K_{S1} is the half-saturation constant associated with the substrate S_1.

Methanogenic Bacteria

In order to emphasize the possible VFA accumulation, we have considered Haldane kinetics for the methanogenesis:

$$\mu_2(S_2) = \mu_{2\max} \frac{S_2}{S_2 + K_{S2} + \frac{S_2^2}{K_{I2}}} \quad (34)$$

where μ_{2max} is the maximum bacterial growth rate without inhibition, and K_{S2} and K_{I2} are the saturation and inhibition constants associated with the substrate S_2, respectively.

THE MODEL STRUCTURE

It is worth noting that the model has a cascade structure. This will make its analysis and its use easier. In this section, we take benefit of this structure to briefly describe the possible behavior of this model, and to discuss the identifiability of its parameters. For the sake of brevity, the mathematical developments are not detailed here.

The Model Behavior

First, we remark that the system of the two Eqs. (20) and (23) can be run separately. It means that S_1 and X_1 are not influenced by the other variables (and, therefore, by the parameters associated with the other equations). This system corresponds to a classical chemostat model (with Monod-type kinetics), with an equivalent mortality rate $k_d = (\alpha - 1)D$ (note that $k_d < 0$). The behavior of such a system is well-known (Smith and Waltman, 1995). For constant influent conditions, two equilibria exist in general. For appropriate values of the dilution rate, the nontrivial equilibrium is stable, and the trivial equilibrium (washout: $X_1 = 0$, $S_1 = S_{lin}$) is unstable.

Note that Eq. (22) (mass balance of Z) is independent of the other equations and can therefore be analyzed separately: as it is a linear equation, it has only one steady state, and this steady state is stable because D is positive.

Similarly, the system composed of Eqs. (20), (23), (21), and (24) can also be considered independently. It can also be noted that the system composed of Eqs. (21) and (24) is a chemostat model (with Haldane-type kinetics), with an influent flow rate $DS_{2in} + k_2\mu_1(\xi)X_1$. The behavior of this model is also well-known (Smith and Waltman, 1995). It has (in the general case) three equilibria: the first one is the interesting operating point, as it is nontrivial and locally stable; the second one is nontrivial and unstable; and the third one is the locally stable trivial equilibrium (washout: $X_1 = 0$, $S_1 = S_{lin}$).

Now, the behavior of the model can be briefly described. Once the system composed of Eqs. (20) and (23) has converged, the variables of Eqs. (21) and (24) will also converge toward one of the two stable equilibria. Finally the dynamical Eq. (25) will drive C toward an equilibrium value.

The Identifiability of the Model Parameters

The first approach for identifying the parameters of a model is to find the set of parameters that minimize a global criterion based on the error between simulated values and measurements. The minimization procedure results in parameter values that give the best fit of the model with the data. Nevertheless, generally speaking, such a global approach poses two problems. The first one is the uniqueness of the obtained parameter values (nonuniqueness means that different sets of parameter values result in an equivalent model behavior). This is the so-called problem of structural identifiability of the model. One has to prove from a theoretical point of view that the parameters can be *uniquely* estimated from ideal measurements. It is only when the uniqueness of the parameters has been shown that it is meaningful to run the global minimization procedure (see, e.g., Dochain et al., 1995). The second problem, related to the practical identifiability of the system, may result from the possible presence of local minima (see, e.g., Vanrolleghem et al., 1995). The minimization algorithm may thus often be trapped into local minima, and this leads to bad parameter estimates. The importance of this phenomenon is directly linked to the number of parameters to be identified, to the informative content of the data, and to the possibly high uncertainty associated with the measurements.

Let us now investigate the structural identifiability of the model. The identifiability problem is a difficult one, and the analysis may be easily cumbersome (Walter and Pronzato, 1997). Here we take advantage of the cascade structure of the model. In particular, the identifiability of the parameters of the subsystem (20), (23) is a classical problem that has been extensively discussed in the literature. If all the state variables are measured, the parameters are identifiable (Chouakri et al., 1994; Holmberg, 1982). We will detail the discussion later on (in the static case) in the case where the biomass is not measured.

The identifiability results also hold for the Haldane-type model described by Eqs. (21) and (24) [note that in that case we can take benefit of the measurement of $q_M(\xi)$].

From total inorganic carbon measurement and using the relationship (13), we can derive k_La. Finally, the identifiability of the parameters k_4 and k_5 associated with the last Eq. (25) follows straightforwardly.

Let us now consider the practical identifiability question. Even if the parameters are identifiable, the considered algorithms may converge toward several values. For this reason, in the sequel we shall *at the same time* describe the identification procedure and discuss the uniqueness of the obtained parameters. With this approach, we shall show that the identification algorithm will provide a unique value, and that the corresponding parameter is identifiable. We shall also show

that, when no biomass measurements are available, the yield coefficients are not identifiable and one can obtain only ratios of yield coefficients.

Principles for Identification

We have split the data set into one set for parameter calibration and one set for parameter validation. One of our primary goals was to have a model able to predict properly the process steady states. Therefore, we have selected a set of steady-state values for parameter calibration. We have then used the data corresponding to the other steady states and to the transients for model validation.

Note that this approach is consistent and perfectly valid from an identification point of view. The model structure is typically composed of the combination of hydrodynamics terms, liquid–gas terms, and conversion (kinetic + yields) terms. The conversion and liquid–gas transfer terms contain all the parameters to be calibrated, while the terms related to the hydrodynamics are typically characterized by the (known) values of the influent and effluent flow rates.

In the next section, the steady-state values of the model variables are computed with respect to the parameters, in order to be used later on in the model identification procedure.

DETERMINATION OF THE MODEL STEADY STATES

Steady-State Values of VFA, COD, and Alkalinity

At steady state, if we do not consider the washout steady state (corresponding to $X_1 = 0$ or $X_2 = 0$), we have from Eqs. (20) and (21):

$$\mu_1(S_1) = \alpha D \tag{35}$$

$$\mu_2(S_2) = \alpha D \tag{36}$$

If $\mu_{1\max} > \alpha D$, this implies from Eq. (33) that S_1^*, the steady-state value of S_1, is equal to:

$$S_1^* = K_1 \frac{\alpha D}{\mu_{1\max} - \alpha D} \tag{37}$$

The possible steady states for S_2 are solutions of Eq. (36). The function $\mu_2(S_2)$ starts growing from 0, reaches a unique maximum, and then decreases to 0. Thus, Eq. (36) admits two solutions (that can reduce to one) only if:

$$\alpha D \leq \max[\mu_2(S_2)]$$

This implies, with the expression (34) of μ_2, that:

$$D \leq \frac{\mu_{2\max}}{\alpha} \frac{\sqrt{K_{I2}}}{\sqrt{K_{I2}} + 2\sqrt{K_{S2}}} \tag{38}$$

Then, the possible steady states for S_2 are solutions of the following equation, deduced from Eqs. (36) and (34):

$$\frac{S_2^2}{K_{I2}} + \left(1 - \frac{\mu_{2\max}}{\alpha D}\right) S_2 + K_{S2} = 0 \tag{39}$$

We denote S_2^* and $S_2^\dagger$ the lowest and the largest solutions of Eq. (39), respectively. We also denote $\mathscr{E}^*$ and $\mathscr{E}^\dagger$ the corresponding equilibria. Note that $\mathscr{E}^\dagger$ corresponds to a steady state in the inhibition phase of the methanogenesis.

The computation of the equilibrium for Z is straightforward from Eq. (22):

$$Z^* = Z_{\text{in}} \tag{40}$$

Steady State of the Biomasses

Using Eqs. (23) and (35), we get:

$$X_1^* = \frac{1}{\alpha k_1}(S_{\text{lin}} - S_1^*) \tag{41}$$

From Eqs. (24), (35), (36), and (41), we have two possible values for X_2:

$$X_2^* = \frac{1}{\alpha k_3}\left(S_{2\text{in}} - S_2^* + \frac{k_2}{k_1}(S_{1\text{in}} - S_1^*)\right) \tag{42}$$

$$X_2^\dagger = \frac{1}{\alpha k_3}\left(S_{2\text{in}} - S_2^\dagger + \frac{k_2}{k_1}(S_{1\text{in}} - S_1^*)\right) \tag{43}$$

Steady State of Gaseous Flow Rates

The value of the methane gas flow rate at steady state in the noninhibitory phase is readily obtained from Eqs. (12) and (36):

$$q_{\text{M}}^* = k_6 \alpha D X_2^* \tag{44}$$

The computation of the carbon gas flow rate is a bit more complicated. Let us first consider Eqs. (13) and (25) at steady state, which give the amount of total inorganic carbon C^* at steady state:

$$q_C^* = k_{\text{L}} a(\text{CO}_2^* - K_{\text{H}} P_{\text{C}}^*) = D(C_{\text{in}} - C^*) + k_4 \alpha D X_1^* + k_5 \alpha D X_2^* \tag{45}$$

We compute C^* with the expression (19), and using Eq. (19), we obtain:

$$\text{CO}_2^* = \frac{1}{k_{\text{L}} a + D}(k_{\text{L}} a K_{\text{H}} P_{\text{C}}^* + D\psi^*) \tag{46}$$

with

$$\psi^* = C_{\text{in}} - Z^* + S_2^* + k_4 \alpha X_1^* + k_5 \alpha X_2^*$$

The relationship (46) between CO_2^* and P_C^* can then be injected in Eq. (14). This gives:

$$K_H P_C^{*2} - \omega^* P_C + P_T \psi^* = 0 \tag{47}$$

where

$$\omega^* = K_H P_T + \psi^* + \frac{k_L a + D}{k_L a} k_6 \alpha X_2^*$$

We know from Eq. (17) that only the lower root is physically admissible. Thus:

$$P_C^* = \frac{\omega^* - \sqrt{\omega^{*2} - 4K_H P_T \psi^*}}{2K_H} \tag{48}$$

The steady-state values CO_2^* and q_C^* can then be directly derived from Eqs. (46) and (14), respectively.

The steady-state values associated with $\mathscr{E}^\dagger$ can be computed by using a similar procedure, and simply by replacing the symbol * by † in Eqs. (44) to (48).

IDENTIFICATION PROCEDURE

Introduction

The model developed in the preceding sections includes thirteen parameters that have to be identified from experimental data. This identification step is very important to guarantee a large validity of the model.

To circumvent these structural and practical identifiability problems, we have chosen an approach based on the following two points. First of all, we have decoupled the estimation into three groups of parameters: the kinetic parameters (μ_{1max}, K_{S1}, μ_{2max}, K_{S2}, K_{I2}, α), the transfer coefficient (k_La), and the yield coefficients (k_i, i = 1 to 6). The motivation for this decoupling lies in the (already mentioned) difficult task of kinetics modeling that usually generates a large uncertainty in bioprocess dynamical models (see also Bastin and Dochain, 1990). We designed therefore the identification procedure in order to estimate each group of parameter independently. The second important point of the identification procedure is the following: We focus on the steady states and we adjust the parameters using linear least-square regressions so as to impose that the model predicts correctly the equilibria reached by the process. The capacity of the model to properly reproduce the transients will then be judged during the validation phase.

During the modeling and identification of the process, we have measured as many process variables as possible (at least for steady-state conditions). We denote $\bar{S}_1$, $\bar{S}_2$, $\bar{Z}$, $\bar{C}$, $\overline{pH}$, $\bar{q}_C$, and $\bar{q}_M$ the mean values of these quantities, measured during a steady-state period. Note that these values correspond to one of the two equilibria $\mathscr{E}^*$ or $\mathscr{E}^\dagger$.

Identification Procedure of the Kinetic Parameters

From Eq. (35), we have the following relationship:

$$\frac{1}{D} = \frac{\alpha}{\mu_{1max}} + K_{S1} \frac{\alpha}{\mu_{1max}} \frac{1}{\bar{S}_1} \tag{49}$$

This relationship can be used with the measurements of the equilibrium values of S_1, $\overline{S}_1$, to estimate the parameters α/μ_{1max} and K_{S1} via a linear regression. Unfortunately, the parameters α and μ_{1max} cannot be distinguished from this relationship. We chose therefore to select values of μ_{1max} from classical bibliographical results (Ghosh and Pohland, 1974).

Equation (36) provides the following relationship:

$$\frac{1}{D} = \frac{\alpha}{\mu_{2max}} + K_{S2} \frac{\alpha}{\mu_{2max}} \frac{1}{\bar{S}_2} + \frac{1}{K_{I2}} \frac{\alpha}{\mu_{2max}} \bar{S}_2 \tag{50}$$

Linear regression then gives the values of the following parameters: α/μ_{2max}, K_{S2}, and K_{I2}. Using the estimated value of α obtained in the previous step, we then get μ_{2max}.

Identification Procedure of the k_La

To estimate the value of the liquid–gas transfer coefficient k_La, we use the relationship (13). The dissolved CO_2 concentration can be computed from the measurement of the total inorganic carbon if we use Eqs. (3) and (5):

$$CO_2 = \frac{C}{1 + \frac{K_b}{[H^+]}} \tag{51}$$

or equivalently:

$$CO_2 = Cf(pK_b, \mathrm{pH}) \tag{52}$$

where $pK_b = -\log_{10}(K_b)$ and f is the function:

$$f(pK_b, \mathrm{pH}) = \frac{1}{1 + 10^{\mathrm{pH} - pK_b}} \tag{53}$$

Then, we get the following expression obtained from Eqs. (13) and (52):

$$q_C = k_L a C f(pK_b, \mathrm{pH}) - k_L a K_H P_C \tag{54}$$

From the measurements of pH, C, flow rate, and partial pressure of CO_2 at steady state, we can now use the following regression to estimate k_La (with K_H = 16 mmol/L per atm):

$$\bar{q}_C = k_L a \left[\overline{Cf}(pK_b, \overline{\mathrm{pH}}) - K_H \bar{P}_C \right] \tag{55}$$

This regression leads to an estimate of k_La.

Identification Procedure of the Yield Coefficients Ratio

The identification of the yield coefficients is performed in two steps. In the first step, four ratios of yield coefficients:

$$\frac{k_6}{k_3}, \frac{k_2}{k_1}, \frac{k_5}{k_3}, \frac{k_4}{k_1} \tag{56}$$

are identified. Then, in a second step, we use the measurements of the VSS to obtain an approximation of each yield coefficient.

We first consider the methane gas flow rate, which we compute by combining Eqs. (42) and (44):

$$\bar{q}_M = D\frac{k_6}{k_3}\left(S_{2in} - \bar{S}_2 + \frac{k_2}{k_1}(S_{1in} - \bar{S}_1)\right) \tag{57}$$

From this regression, we get the ratio of yield coefficients k_6/k_3 and k_2/k_1.

From the consideration of the CO_2 flow rate (45), using Eqs. (41) and (42), we obtain:

$$\bar{q}_C = D\left[C_{in} - \bar{C} + \left(\frac{k_4}{k_1} + \frac{k_5}{k_3}\frac{k_2}{k_1}\right)(S_{1in} - \bar{S}_1) + \frac{k_5}{k_3}(S_{2in} - \bar{S}_2)\right] \tag{58}$$

We rewrite this equation as follows:

$$\frac{\bar{q}_C}{D} - (C_{in} - \bar{C}) = \frac{k_4}{k_1}(S_{1in} - \bar{S}_1) + \frac{k_5}{k_6}\frac{\bar{q}_M}{D} \tag{59}$$

This regression gives the values of k_4/k_1 and k_5/k_6.

Determination of the Yield Coefficients

In this second step, we show how to estimate each yield coefficient. It turns out that the yield coefficients are not identifiable if we do not measure the biomasses. Indeed, it can be verified that if we rescale the biomass by the factors λ_1 and λ_2,

$$X_1' = \lambda_1 X_1 \tag{60}$$

$$X_2' = \lambda_2 X_2 \tag{61}$$

then the biomass rescaling can be compensated by the following parameter rescaling:

$$k_1' = \frac{k_1}{\lambda_1}, \quad k_2' = \frac{k_2}{\lambda_1}, \quad k_4' = \frac{k_4}{\lambda_1} \tag{62}$$

$$k_3' = \frac{k_3}{\lambda_2}, \quad k_5' = \frac{k_5}{\lambda_2}, \quad k_6' = \frac{k_6}{\lambda_2} \tag{63}$$

The numerical simulation of the model with the yield coefficients k_i and k_i' will give the same values for all the model variables (except for the variables X_1 and X_2 that are not measured). The yield coefficients are not identifiable if no measurements of the biomass is available; this is consistent with the study of Chappell and Godfrey (1992), who proved a similar result when only the biomass is measured.

This means that all the variables but the biomasses depend only on the ratio of yield coefficients. The values of the yield coefficients themselves (and not of their ratio) are then needed only if we want to have an estimate of the biomasses in the fermenter.

For that purpose, we need additional information and measurements related to the biomasses. We propose first to use the ratio ν of acidogenic and methanogenic bacteria. This information is quite qualitative and can be determined despite the heterogeneity between the liquid and the solid phases. We propose also to use the VSS concentration as a (rough) indicator of the total biomass $X_1 + X_2$.

From Eqs. (41) and (42) we have:

$$\nu = \frac{\bar{X}_1}{\bar{X}_1 + \bar{X}_2} \simeq \frac{1}{\alpha k_1}\frac{S_{1in} - \bar{S}_1}{\overline{VSS}} \tag{64}$$

If we assume that ν remains approximately constant, we finally have an estimate of k_1:

$$k_1 = \frac{1}{\alpha\nu}\frac{S_{1in} - \bar{S}_1}{\overline{VSS}} \tag{65}$$

The value of ν has been taken from the literature ($\nu = 0.2$) (Sanchez et al., 1994).

Now, if we consider Eqs. (41) and (42), we have:

$$\nu = \frac{\bar{X}_1}{\bar{X}_1 + \bar{X}_2} = \frac{k_3}{k_1}\frac{S_{1in} - \bar{S}_1}{(S_{2in} - \overline{S}_2) + (\frac{k_2}{k_1} + \frac{k_3}{k_1})(S_{1in} - \overline{S}_1)} \tag{66}$$

and thus:

$$k_3 = k_1\frac{\nu}{1-\nu}\left(\frac{S_{2in} - \bar{S}_2}{S_{1in} - \bar{S}_1} + \frac{k_2}{k_1}\right) \tag{67}$$

An estimate of k_3 can then be found from Eq. (67). The ratios identified in the previous step can now be used to derive estimates of k_2, k_4, k_5, and k_6.

Note that these values have to be considered with care because of the uncertainty of the VSS measurements, the uncertainty of the ratio of methanogenic and acidogenic bacteria, and, last but not least, the uncertainty of the correlation between the total biomass and the VSS.

Sensitivity Analysis

In this section, we study the sensitivity of the model to its parameters. Note that there does not exist any methodology to discuss the parameter sensitivity in general: The usual methods refer to parameter sensitivity *for a given system trajectory* (i.e., in reference to a given set of parameters, initial conditions, and influent flow rates). Therefore, it is of great importance to correctly choose the reference simulation from which the sensitivity analysis is performed. This results in fact from an iterative approach, where the "best parameter

values'' serve as a basis to run the sensitivity analysis. The classical choice is to consider the sensitivity coefficient σ_y^p of the variable y to the parameter p defined by $\sigma_y^p = \partial y/\partial p$ (Walter and Pronzato, 1997). These quantities are computed by running the adjoint dynamical system. The drawback of this method is that it gives an idea of the sensitivity *for small parameter variations*. In order to explore the effect of large parameter variation, we use the following criterion for experiment from time 0 to t_f:

$$\sigma_y^{\Delta p} = \frac{1}{t_f}\int_0^{t_f} \frac{y(p+\Delta p, x_0, u, \tau) - y(p, x_0, u, \tau)}{y(p, x_0, u, \tau)} d\tau$$

where $y(p, x_0, u, \tau)$ denotes the simulated value at time τ of the variable y associated with the parameter p, the initial condition x_0, and the input u.

In the sequel, we have focused the discussion on the sensitivity of the four following quantities to parameter variations: S_1, S_2, q_C, and q_M.

The results are presented in Fig. 3. Note first that the cascade model structure has a strong influence on the parameter sensitivity. Indeed, the only parameters influencing S_1 are μ_{1max}, K_{S1}, k_1, and α. The parameters influencing S_2 are those influencing S_1 plus μ_{2max}, K_{S2}, K_{I2}, k_2, and k_3. These parameters (plus k_6) also influence q_M. Finally, all the parameters act on q_C. Nevertheless, the influence of the parameters only related to S_1 is much lower on S_2 and on the gaseous flow rates. Similarly, the parameters influencing S_2 have less effect on q_C.

From this study, it results that the parameters that played the main role are α (because it modifies the dynamics of the whole model) and k_3 (which has a strong influence on the gaseous flow rates). Note that the small values of μ_{2max} and K_{I2} also strongly change the model predictions: with low value the equilibrium S_2^* becomes less and less stable.

The parameters k_2, k_4, k_La, K_{S_1} and K_{S_2} have little influence on the model, and therefore they will be less precisely estimated.

Finally, it can be noted that sensitivity analysis (in %) for the ratio of yield parameters k_i/k_j is the same as that of k_i (in %).

Identification of Parameter Values from Experimental Data

As already mentioned, the data have been split in two sets. The first set, composed of a set of values obtained at equilibrium (after a sufficiently long time after the dilution rate and the wastewater composition has been changed), has been used for the calibration, and the remaining set of data is kept for the validation. The steady-state values are averaged over the considered period, then the obtained averaged values are used for the regressions. The characteristics of the influent during the considered periods are presented in Table II. The estimated standard deviation for some parameters is quite high. However, this value is probably overestimated if we keep in mind the relatively small number of equilibria (seven points) from a statistical point of view. Note also that the deviations are particularly high for two classes of parameters. First, the estimates of the kinetic coefficients suffer from the already mentioned lack of reliability of the kinetic expression used. Indeed, the fact that the expressions retained for the biological kinetics are only rough approximations results in high variability of the corresponding parameter values. The other group of parameters for which the estimates seem to be less precise are the ratio of parameter related to k_1 (k_2/k_1 and k_4/k_1). This is probably due to the fact that the composition of the substrate S_1 is changing throughout the experiment. As a consequence, the yield coefficient associated to its degradation (i.e., k_1) may fluctuate during the considered period. As we shall see in the sequel, in spite of this apparent uncertainty, the model correctly fits the data.

Tables III and IV summarize the obtained kinetic parameters and yield coefficient ratio values. Table V then gives the values obtained for all the yield coefficients.

Table II. Mean influent characteristics used for steady-state identification.

D (d^{-1})	COD_{in} (g/L)	VFA_{in} (mmole/L)	pH_{in}
0.34	9.5	93.6	5.12
0.35	10	73.68	4.46
0.35	4.8	38.06	4.49
0.36	15.6	112.7	4.42
0.26	10.6	72.98	4.42
0.51	10.7	71.6	4.47
0.53	9.1	68.78	5.30

Table III. Estimates of the kinetic parameters.

Parameter	Meaning	Unit	Value	SD[a]
μ_{1max}	Maximum acidogenic biomass growth rate	d^{-1}	1.2[b]	
K_{S1}	Half-saturation constant associated with S_1	g/L	7.1	5.0
μ_{2max}	Maximum methanogenic biomass growth rate	d^{-1}	0.74	0.9
K_{S2}	Half-saturated constant associated with S_2	mmol/l	9.28	13.7
K_{I2}	Inhibition constant associated with S_2	mmol/l	256	320
α	Proportion of dilution rate for bacteria	mmol/l	0.5	0.4
k_La	Liquid/gas transfer rate	d^{-1}	19.8	3.5

[a]SD = standard deviation.
[b]From Ghosh and Pohland (1974).

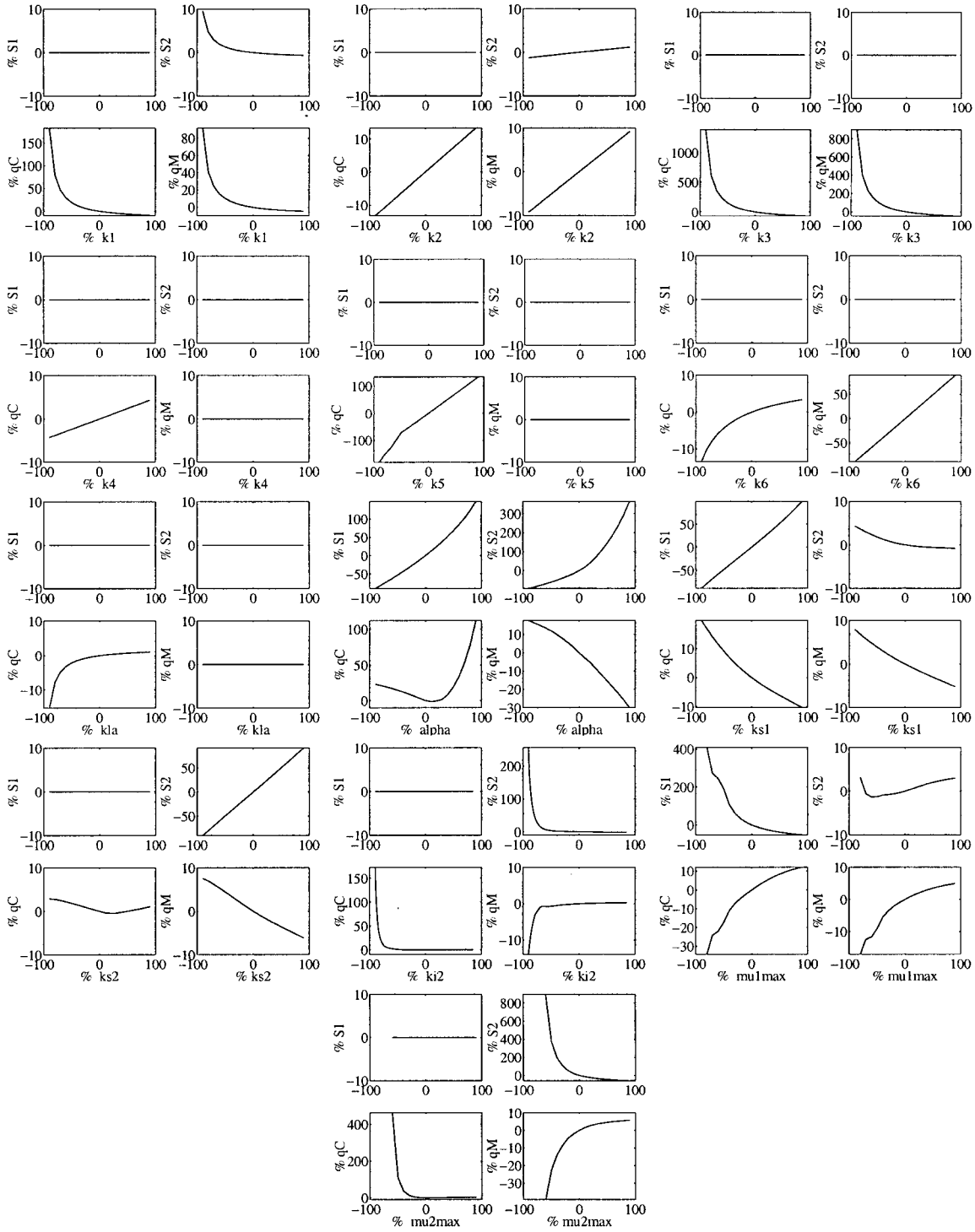

Figure 3. Sensitivity for the model parameters. The mean changes of S_1, S_2, q_C, and q_M are represented with respect to the deviation of the nominal value of the considered parameter.

MODEL VALIDATION

The simulation results are presented in Figs. 4, 5, and 6. The periods of time considered for the calibration step are shown on the figures. The initial conditions used to initiate the simulation have been estimated by computing the equilibrium obtained with the initial values of influent concentrations and pH.

The model correctly reproduces the behavior of the system for the considered period, in spite of the fact that

Table IV. Estimates of the yield coefficient ratios.

Ratio	Unit	Value	SD[a]
$k2/k_1$	mmol/g	2.72	2.16
$k6/k_3$		1.62	0.12
$k5/k_3$		1.28	0.13
$k4/k_1$	mmol/g	1.18	3.02

[a] SD = standard deviation.

it has been calibrated only using steady-state measurements.

Indeed, Fig. 4 shows that the continuously measured variables (i.e., gaseous flow rate and pH) are well predicted. It is worth noting that these simulations also correctly reproduce the effect of the disturbances induced by pump failures (around day 45). We remark also that the pH predictions match quite well the direct measurements, although pH measurements have not been used to calibrate the model parameters. However, the model predicts a more severe pH drop during the destabilization phase (days 21–25). This may be due to an underestimation of the buffer capacity (i.e., the alkalinity of the system). It can be noticed that during the destabilization period, the gases are underestimated by the model.

The model simulations are also in good agreement with the offline data (Fig. 5). Even if S_1 is a variable that stands for the various components of the COD that can be rather different along the experiment, the adequacy between model and measurements is good. The peak of S_1 measured around day 50 is not represented by the model. However, this peak is difficult to explain from a biochemical viewpoint, because it does not correspond to an increase of the organic loading rate. Moreover, it does not coincide with an increase of volatile fatty acid. The reaction of the model to the overloading produced on day 68 seems to be slower than the process, so that the accumulation starts less rapidly in the model.

Similar conclusions can be drawn for the volatile fatty acids for which the model predictions match fairly well the measurements. The fact that the model reacts less rapidly than the process for overloading can also be noticed around day 68.

For the simulations of alkalinity and total inorganic carbon, there exists a bias compared to the data. This is probably due to the uncertainty attached to the uncertain measurement of the influent alkalinity. Indeed, the

Table V. Estimates of the yield coefficients.

Parameter	Meaning	Unit	Value	SD[a]
k_1	Yield for COD degradation		42.14	18.94
k_2	Yield for VFA production	mmol/g	116.5	113.6
k_3	Yield for VFA consumption	mmol/g	268	52.31
k_4	Yield for CO_2 production	mmol/g	50.6	143.6
k_5	Yield for CO_2 production	mmol/g	343.6	75.8
k_6	Yield for CH_4 production	mmol/g	453.0	90.9

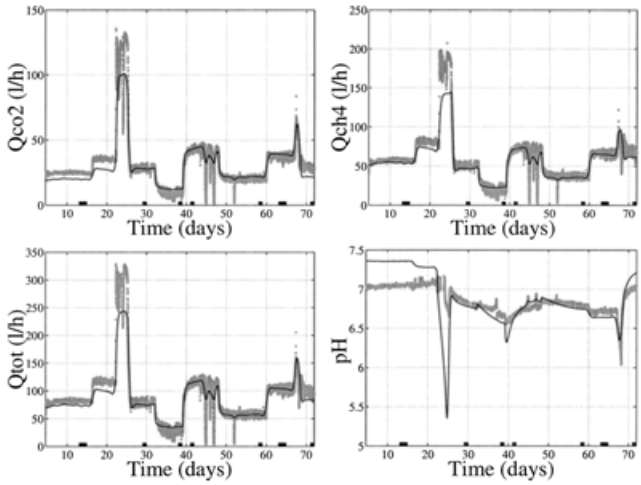

Figure 4. Comparison between simulation results and measurements for the gaseous flow rates and the pH. The periods considered for the calibration step are represented on the time axis.

influent total alkalinity titration is less precise, because the pH in the influent is low.

Finally, the comparison between the measured VSS and the simulated total biomass (*i.e.*, $X_1 + X_2$) is presented in Fig. 6. The main trends of the data are respected even if the correlation between VSS and biomass is probably poor. The peak of VSS during the destabilization period is probably not due to a biomass increase.

The main quality of the model is its ability to predict the destabilization of the plant. This was not obvious, because only equilibrium data have been used for the model calibration and the data obtained during the destabilization phases were not used. The quality of the model justifies its integration in an online monitoring procedure, in order to early detect a possible destabilization (Bernard et al., 1999). The model is also used to derive a robust control algorithm that is insensitive to

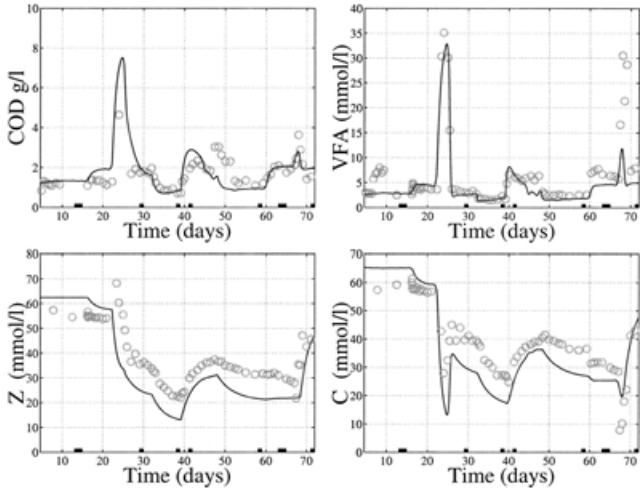

Figure 5. Comparison between simulation results and measurements for COD, VFA, alkalinity, and total inorganic carbon. The periods considered for the calibration step are underlined.

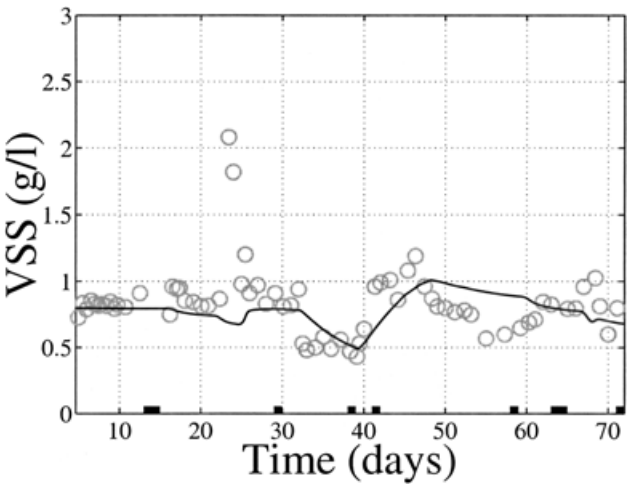

Figure 6. Comparison between measured VSS and simulated total biomass ($X_1 + X_2$). The periods considered for the calibration step are underlined.

the main modeling uncertainties and that avoids the plant destabilization (Bernard et al., 2001).

CONCLUSION

In this paper, we have built, identified, and validated a model for an anaerobic treatment plant. The four following points are important, because they guarantee that our model can be useful to monitor and control the anaerobic process.

1. It is based on mass-balance considerations. The modeling uncertainty due to the variability of the biological kinetics is concentrated in the reaction rates terms.
2. An identification procedure privileging the steady-state predictions has been developed which allows identification of all the parameters of the model and understanding of the role played by the parameters in the process dynamics.
3. Experiments have been designed, covering a wide range of experimental conditions, in order to develop and validate the model. This diversity is obtained via various organic loading rates (given by various dilution rates and various influent COD concentrations), but it also results from a wide range of substrate compositions, because the vinasses used during the experiment do not all have the same origin.
4. The validation of the model has been performed for a broad set of transient conditions. The model that was identified during steady states proves to be efficient in dynamical conditions, in particular during the destabilization phases.

This paper includes results of the project AMOCO, which is supported by the Agriculture & Fisheries program (FAIR) of the European Community (Contract ERB-FAIR-CT96-1198). It also presents research results of the Belgian Programme on Inter-University Poles of Attraction, initiated by the Belgian State, Prime Minister's office for Science, Technology, and Culture. The scientific responsibility rests with its authors.

NOMENCLATURE

B	bicarbonate concentration (mmol/L)
C, C_{in}	total inorganic carbon concentration (mmol/L)
D	dilution rate (d^{-1})
d/dt	time derivative
k_1	yield for substrate degradation
k_2	yield for VFA production (mmol/g)
k_3	yield for VFA consumption (mmol/g)
k_4	yield for CO_2 production (mmol/g)
k_5	yield for CO_2 production (mmol/g)
k_6	yield for CH_4 production (mmol/g)
K_a, K_b	equilibrium constants (mol/L)
K_H	Henry's constant (mmol/L per atm)
k_La	liquid–gas transfer constant (d^{-1})
K_{I2}	inhibition constant (mmol/L)
K_{S1}	half-saturation constant (g/L)
K_{S2}	half-saturation constant (mmol/L)
P_C	CO_2 partial pressure (atm)
P_T	total pressure (atm)
q_C	carbon dioxide flow rate (mmol/L per d)
q_M	methane flow rate (mmol/L per d)
r, r_1, r_2	reaction rates (d^{-1})
S_1, S_{1in}	organic substrate concentration (g/L)
S_2, S_{2in}	volatile fatty acids concentration (mmol/L)
X_1	concentration of acidogenic bacteria (g/L)
X_2	concentration of methanogenic bacteria (g/L)
Z, Z_{in}	total alkalinity (mmol/L)
Z_0	anion concentration (mmol/L)
α	fraction of bacteria in the liquid phase
ν	mean fraction of acidogenic bacteria
μ_1	specific growth rate of acidogenic bacteria (d^{-1})
μ_{1max}	maximum acidogenic bacteria growth rate (d^{-1})
μ_2	specific growth rate of mathanogenic bacteria (d^{-1})
μ_{2max}	maximum methanogenic bacteria growth rate (d^{-1})
ξ	vector of the process variables

References

Andrews J. 1968. A mathematical model for the continuous culture of microorganisms utilizing inhibitory substrates. Biotechnol Bioeng 10:707–723.

Bastin G, Dochain D. 1990. On-line estimation and adaptive control of bioreactors. Amsterdam: Elsevier.

Batstone D, Keller J, Newell B, Newland M. 1997. Model development and full scale validation for anaerobic treatment of protein and fat based wastewater. Water Sci Technol 36:423–431.

Bernard O, Hadj-Sadok Z, Dochain D. 1999. Dynamical modelling and state estimation of anaerobic wastewater treatment plants. In: Proceedings of ECC99 (CD-ROM). Germany: Karlsruhe.

Bernard O, Polit M, Hadj-Sadok Z, Pengov M, Dochain D, Estaben M, Labat P. 2001. Advanced monitoring and control of anaerobic wastewater treatment plants: Software sensors and controllers for an anaerobic digestor. Water Sci Technol 43(7): 175–182.

Chappell M, Godfrey KR 1992. Structural identifiability of the parameters of a nonlinear batch reactor model. Math Biosci 108:241–251.

Chouakri N, Fonteix C, Marc I, Corriou J. 1994. Parameter estimation of a Monod-type model. Part I: Theoretical identifiability and sensitivity analysis. Biotech Tech 8:683–688.

Costello D, Greenfield P, Lee P. 1991a. Dynamic modelling of a single-stage high-rate anaerobic reactor—I. Model derivation. Water Res 25:847–858.

Costello D, Greenfield P, Lee P. 1991b. Dynamic modelling of a single-stage high-rate anaerobic reactor—II. Model verification. Water Res 25:859–871.

Dochain D, Perrier M, Pauss A. 1991. Adaptive control of the hydrogen concentration in anaerobic digestion. Ind Eng Chem Res 30:136–141.

Dochain D, Vanrolleghem P, Daele MV. 1995. Structural identifiability of biokinetic models of activated sludge respiration. Water Res 29:2571–2578.

Fernandes L, Kennedy K, Ning Z. 1993. Dynamic modelling of substrate degradation in sequencing batch anaerobic reactors (SBAR). Water Res 27:1619–1628.

Fripiat J, Bol T, Binot R, Nyns E. 1984. A strategy for the evaluation of methane production from different types of substrate biomass. Exeter, UK: Roger Bowskill Ltd. pp 95–105.

Ghosh S, Pohland F. 1974. Kinetics of substrate assimilation and product formation in anaerobic digestion. J Water Pollut Control Fed 46:748–759.

Graef S, Andrews J. 1974. Mathematical modeling and control of anaerobic digestion. Water Res 8:261–289.

Hill D, Barth C. 1977. A dynamic model for stimulation of animal waste digestion. J Water Pollut Control Assoc 10:2129–2143.

Holmberg A. 1982. On the practical identifiability of microbial growth models incorporating Michaelis-Menten type nonlinearities. Math Biosci 102:41–73.

Kiely G, Tayfur G, Dolan C, Tanji K. 1997. Physical and mathematical modelling of anaerobic digestion of organic wastes. Water Res 31:534–540.

Mata-Alvarez J, Macé S, Llabres P. 2000. Anaerobic digestion of organic solid wastes. An overview of research achievements and perspectives. Bioresour Technol 74:3–16.

Moletta R, Verrier D, Albagnac G. 1986. Dynamic modelling of anaerobic digestion. Water Res 20:427–434.

Mosey F. 1983. Mathematical modelling of the anaerobic digestion process: Regulatory mechanisms for the formation of short-chain volatile acids from glucose. Water Sci Technol 15:209–232.

Pavlostathis SG. 1994. Anaerobic processes. Water Environ Res 44:342–356.

Perrier M, Dochain D. 1993. Evaluation of control strategies for anaerobic digestion processes. Int J Adapt Contr Sign Proc 7:309–321.

Ripley LE, Boyle JC, Converse JC. 1986. Improved alkalimetric monitoring for anaerobic digestion of high-strength wastes. J Water Pollut Control Fed 58:406–411.

Rozzi A. 1984. Modeling and control of anaerobic digestion processes. Trans Inst Meas Control 6:153–159.

Sanchez J, Arijo S, Muñoz M, Moriñigo, M, Boirrego J. 1994. Microbial colonization of different support materials used to enhance the methanogenic process. Appl Microbiol Biotechnol 41:480–486.

Smith HL, Waltman P. 1995. The theory of the chemostat: Dynamics of mocrobial competition. Cambridge, UK: Cambridge University Press.

Steyer JP, Buffiere P, Rolland D, Moletta R. 1999. Advanced control of anaerobic digestion processes through disturbances monitoring. Water Res 9:2059–2068.

Vanrolleghem P, Daele MV, Dochain D. 1995. Practical identifiability of a biokinetic model of activated sludge respiration. Water Res 29:2561–2570.

Walter E, Pronzato L. 1997. Identification of parametric models. Springer-Verlag: Berlin.